Published in final edited form as:
J Am Chem Soc. 2006 April 19; 128(15): 4992–5000. doi:10.1021/ja056613z.

Analysis of Human Telomerase Activity and Function by Two Color Single Molecule Coincidence Fluorescence Spectroscopy

Xiaojun Ren, **Haitao Li**, **Richard W. Clarke**, **David A. Alves**, **Liming Ying**, **David Klenerman***, and **Shankar Balasubramanian***
Department of Chemistry, University of Cambridge, Lensfield Road, Cambridge CB2 1EW, U.K.

Abstract

Telomerase is a nonclassical DNA polymerase that uses its integral RNA as a template to synthesize telomeric repeats onto chromosome ends. The molecular mechanism of telomerase is unique and involves a translocation step after the synthesis of each telomeric repeat. To directly measure the enzymatic turnover of substrate and the efficiency of the translocation step we have extended our two-color single molecule fluorescence coincidence method. The method employs Cy5-dATP incorporation into a DNA primer that has been prelabeled with a reference fluorophore. Measurements are performed in the single molecule regime and products, which necessarily have both fluorophores, are excited by two independent lasers, and give rise to coincident events. By counting the number of coincident events and using the coincidence detection efficiency, it is possible to determine the number of the extended products generated by attomole quantities of telomerase, without separation or the use of PCR or radioactivity. Histograms of the logarithms of the ratios of the Cy5 to the reference fluorophore fluorescence can be used to determine the length distribution of the products and hence the enzyme processivity. The mean processivity obtained from the single molecule fluorescence coincidence assay is 0.32 ± 0.04, in good agreement with the value of 0.37 ± 0.05 derived from the direct radioactive assay approach. The function of the alignment domain of human telomerase RNA in sustaining catalytic activity in vitro has been reevaluated using this method. Together with our previous results these experiments identify the essential residues in the alignment domain of human telomerase RNA that contribute to the activity and processivity of telomerase.

Introduction

Telomerase is responsible for the synthesis of DNA repeats that make up the telomeres at chromosome ends. Telomerase function is fundamental to the proliferation and differentiation of cells, and has been directly linked to various diseases that include cancer1,2 and stem cell disorders.3-5 Catalytically active telomerase minimally comprises protein (hTERT for human) and RNA (hTR for human).6 In particular, there is direct involvement of the RNA component in the catalytic mechanism whereby a segment of RNA actually templates the synthesis of telomeric DNA repeats, $(TTAGGG)_n$ in humans. The proposed molecular mechanism for human telomerase (Figure 1) involves initial binding of DNA primer to the active site via base-pairing interactions with the template domain of hTR and an additional interaction with the anchor site in the hTERT subunit. Nucleotides are then incorporated until the extended DNA primer reaches the 5′-boundary of the template. After

*E-mail: dk10012@cam.ac.uk; sb10031@cam.ac.uk.

Supporting Information Available: Justification of the use of normal distributions to fit histograms of logarithms of ratios of fluorescences of intensities from coincidence events; complete author list of ref 25. This material is available free of charge via the Internet at http://pubs.acs.org.

Europe PMC Funders Author Manuscripts

one repeat addition, the extended DNA either dissociates from the RNA template, terminating the synthesis, or the DNA undergoes a dynamic process, i.e., translocation, repositioning it back to the beginning of the RNA template ready for another round of telomere DNA synthesis.6 Translocation is a distinct mechanistic feature of telomerase. Human telomerase can add several repeats to a DNA primer prior to a dissociation event, and is consequently said to have high *processivity*.7 The efficiency of the translocation step will depend on the ratio of rate constants for translocation (k_{trans}) to DNA product dissociation (k_{off}) (Figure 1), and this will determine the processivity and the length distribution of products. To study the mechanism of telomerase in detail, it is therefore critical to be able to quantify the products of catalysis and also measure the translocation efficiency.

Numerous approaches for measuring telomerase activity have been reported. The major challenges being faced are the relatively minute quantities of telomerase enzyme available plus the need to quantitate a mixture of extended products of varying lengths. The PCR-based telomeric repeat amplification protocol (TRAP) assay is the most widely used method.1,8 TRAP is very sensitive, but suffers from numerous artifacts from the PCR-associated amplification procedure, that include altering the length distribution of telomerase products, false positive and negative results, and primer dimer issues9,10 making it difficult to reliably characterize mechanistic details. Moreover, the TRAP assay cannot detect very short telomerase products and consequently cannot characterize cases where the enzyme operates with low processivity.11 The direct primer extension assay11-13 is a powerful method, but requires relatively large quantities of purified, concentrated enzyme and high levels of radioactivity. The TRAP and direct assays each generally require electrophoretic separation of telomeric products. A number of nonradioactive assay methodologies have been developed more recently,14-16 but these methods only provide a simple measure of relative total activity and do not report on the processivity of the enzyme.

Fluorescence spectroscopy has been employed to analyze biomolecules in the single molecule regime to avoid the need for separation, as is required for ensemble methods.17 In solution, experiments are usually performed using a tightly focused Gaussian laser beam to define a small, subfemtoliter, confocal volume. Molecules that pass through different parts of the laser beam are subjected to different intensities and hence produce a broadened distribution of fluorescence intensities. To remove the effect of the inhomogeneity of the excitation source, two ratiometric methods have been employed.17,18 The first method is fluorescence resonance energy transfer (FRET)19 which requires one-color excitation and two-color detection, and the second method is two-color coincidence detection (TCCD),18 that requires two-color excitation and two-color detection. In both cases the ratio of fluorescence from the two fluorophores, on the same molecule or complex, is used to make the single molecule measurement. TCCD has the advantage, exploited in this work, that the intensity of the fluorescence from the two types of fluorophores does not depend on their intramolecular separation but only on the number of fluorophores present, provided there is no significant quenching. Previous ratiometric studies of molecular conformation and molecular complexes have used a particular function of the fluorescence intensities of the two fluorophores, $I_1/(I_1 + I_2)$, which evaluates to a number between 0 and 1. This function is widely used for FRET studies. Peaks in its probability density follow gamma distributions but are approximately Gaussian when their central peaks are away from 0 or 1. This function is therefore easily applicable to TCCD when there are less than three fluorophores present so that the normalized ratio is also not close to 0 or 1. However, in this work up to six fluorophores of one type can be present in one molecule, and in this regime the function $I_1/(I_1 + I_2)$ cannot precisely discriminate between separate peaks if constant width binning is employed. It is far easier to work with the method we propose in this paper, which uses an alternative function, $\ln(I_{red}/I_{blue})$, and constant width binning. This method was first

validated using a mixture of model samples of known fluorophore stoichiometries and then was exploited to directly count the number of extended products formed by telomerase and thus characterize telomerase function.

Experimental Section

SamplesandPlasmids

Theprimer(5′-GGTT*AGGGTTAGGGTTAGGG-3′, T* labeled with Alexa-488) was synthesized by IBA GmbH and purified by polyacryamide gel electrophoresis. Analysis by UV absorbance confirmed (>98%) Alexa-488 labeling efficiency. The cyanine 5-dATP (Cy5-dATP) was purchased from Perkin-Elmer with >95% of chemical purity. The plasmids pET28a-hTERT, pUC18-hTR+1, and pUC18-hTR Sub3 (^{56}CAA^{54} substituted by GTT) variant have been previously described.20 The 5′-end labeled hTR was prepared as previously described.21 The 40-bp single-stranded oligonucleotide (5′-(Cy5)T*ACCGATTACTGGCTCTTATCCTAGGCTTAAGTTACACTA-3′ and 5′-(Alexa-488)T*AGTGTAACTTAAGCCTAGGATAAGAGCCAGTAATCGGTA-3′ (T* designates a dye-labeled nucleotide)) were obtained from IBA GmbH. The duplex used for measurement of coincidence detection efficiency was obtained by annealing the two single-stranded dye-labeled oligonucleotides.

Model Samples

HPLC-purified 40-base oligonucleotide 5′-TAG TGT AAC TTA AGC CTA GGA TAA GAG CCA GTA ATC GGT A-3′ (MWG-Biotech, Ebersberg, Germany) and 80 base oligonucleotide, composed of two repeats of the 40 base sequence, 5′-TAG TGT AAC TTA AGC CTA GGA TAA GAG CCA GTA ATC GGT ATA GTG TAA CTT A AG CCT AGG ATA AGA GCC AGT AAT CGG TA-3′ (IBA GmbH, Goettingen Germany) were 5′-labeled with the fluorophore Rhodamine Green (RG) (maximum emission at 532 nm). The complementary 40-base oligonucleotide having a 5′ 6-carbon amino modifier (Transgenomics, UK) was desalted (NAP 5 column, Amersham, UK) and labeled with an Alexa-647 (maximum emission at 666 nm) oligonucleotide amine labeling kit (Molecular Probes) following the manufacturer's instructions. The labeled oligonucleotide was separated from the excess dye by gel filtration using a Sephadex 25 (Amersham, UK) column followed by ethanol precipitation, and then from unlabeled DNA by denaturing gel electrophoresis (20% acrylamide, 8 M urea and 1 × TBE with a 1 × TBE running buffer). The bands containing labeled oligonucleotide were identified by visual inspection and UV shadowing. They were excised, and the DNA was eluted into 10 mM Tris·HCl pH 7.4 using the "crush and soak" method. The oligonucleotide was purified by extraction with phenol:chloroform:isoamyl alcohol 25:24:1, ethanol precipitation and desalting with a NAP 5 column. Double-stranded DNA (dsDNA) samples were prepared by mixing the 40mer with its complementary 40mer or the 80mer with two equivalents of the 40mer complementary strand, heating to 90 °C, and slowly cooling to room temperature to form duplex. Bulk measurements showed no FRET for either structure.

Production of Cy5-Alexa-488 Single-Stranded Extension Product

The template used for Klenow fragment extension was obtained by annealing two single-stranded DNAs of 5′-GGTT*(Alexa-488)-AGGGTTAGGGTTAGGG-3′ (T* designates a dye-labeled nucleotide) and 5′-GGGATTCCCTAACCCTAACCCTAACC-3′. The extension was carried out in 50-μL volume in buffer containing 10 mM Tris-HCl, pH 7.9, 50 mM NaCl, 10 mM $MgCl_2$, 1 mM DTT, 40 μM dCTP, 40 μM dATP, 40 μM Cy5-dUTP, 10 U Klenow fragment (BioLabs), and 100 nM template. The reaction mixture was incubated at 37 °C for 3 h in a water bath. The reaction was stopped by adding 150 μL of TEN buffer (10 mM Tris-HCl, 1 mM EDTA, and 300 mM NaCl), and the mixture was

Europe PMC Funders Author Manuscripts

extracted with equal volume of phenol/chloroform. The supernatant was applied three times to G-25 spin columns to remove excess nucleotides and was dialyzed twice against 800 mL of autoclaved TEN buffer using a MicroDispoDialyzer (MWCO 3.5 kDa, Spectrum Laboratories). To release single-stranded Cy5-Alexa-488 DNA, 100-fold excess antisense oligonucleotide was added, heated at 95 °C for 5 min, and slowly cooled to room temperature.

Construction of pET28a-hTERT-3×FLAG Plasmid

The pET28a-hTERT plasmid was amplified by PCR to change the stop codon of hTERT gene using the forward primer 5′-AAAGGAATTCCATATGCCGCGCGCTCCCCG-3′ and the reverse primer 5′-CCGGAATTCTGAGTCCAGGATGGTCTTGAA-3′ containing *Nde* I and *EcoR* I restriction sites respectively (underlined). The PCR fragments were digested with *Nde* I and *EcoR* I and subsequently cloned into pET28a-hTERT digested with the same enzymes. The sense strand, 5′-CGGAATTCGACTACAAAGACCATGACGGTGATTATAAAGA TCATGACATCGATTACAAGGATGACGATGACAAGTAAGCGGCCGCAAAAGGAA AA-3′ (*EcoR* I site underlined) (Invitrogen), and the antisense strand, 5′-TTTTCCTTTTGCGGCCGCTTACTTGTCA TCGTCATCCTTGTAATCGATGTCATGATCTTTATAATCA-CCGTCATGGTCTTTGTAGTCGAATTCCG-3′ (*Not* I site underlined) (Invitrogen) were mixed at equal molarity in TE buffer (10 mM Tris-HCl, 1 mM EDTA), heated at 95 °C for 5 min, and then slowly cooled to room temperature for 60-90 min to form dsDNA that encodes the 3×FLAG sequences. The dsDNA was digested with *Not* I and *EcoR* I and subsequently cloned into pET28a-hTERT (stop codon changed) digested with the same enzymes. The identity of the final construct, pET28a-hTERT-3×FLAG, was confirmed by sequencing.

In Vitro Reconstitution of Telomerase

Active telomerase was reconstituted in rabbit reticulocyte lysate (RRL) in the presence of in vitro transcribed hTR and hTERT mRNA, as described previously.20 Briefly, hTERT mRNA and hTR were each produced by in vitro transcription of linearized plasmid using T7 RNA polymerase. Telomerase activity was reconstituted using the nuclease-treated RRL (Promega) at 70% final concentration complemented with purified hTERT mRNA transcripts (25 ng/μL lysate) and wild type or hTR variants (0.1 μg/mL lysate). To quantify the concentration of purified telomerase by single molecule measurement, telomerase was reconstituted in the presence of hTR 5′-end labeled by Alexa-488 (100 nM) and hTERT-3×FLAG mRNA transcripts (25 ng/μL lysate) as described above.

Immunopurification of Recombinant Telomerase

3×FLAG-tagged telomerase in RRL was immunoprecipitated by anti-FLAG M2 affinity agarose beads (Sigma) and eluted by 3×FLAG peptide (Sigma). The beads (40 μL) were washed three times in 0.5 mL of wash buffer (50 mM Tris-HCl, pH 7.4, 150 mM NaCl, 1 mM EDTA, 5 mM $MgCl_2$, 10 mM potassium glutamate, 1% glycerol, and 0.1% Nonidet P-40) and centrifuged at 1500*g* for 2 min between each wash. The beads were incubated twice with 0.5 mL of blocking buffer (wash buffer plus 0.5 mg/mL lysozyme, 0.5 mg/mL BSA, 0.05 mg/mL glycogen, and 0.1 mg/mL yeast tRNA) for 30 min at 4 °C. Reconstituted telomerase (200 μL) was added to 200 μL of blocking buffer and centrifuged at 13000*g* for 20 min at 4 °C to remove any precipitate. The supernatant was added to 40 μL of blocked beads and agitated for 3 h at 4 °C. The beads were washed four times in 0.5 mL of wash buffer and incubated with 200 μL of elution buffer (wash buffer plus 50 ng/μL 3×FLAG peptide) for 1 h at 4 °C.

Telomerase Primer Extension Using Labeled dATP

The primer extension was carried out in 25 μL of volume in buffer containing 50 mM Tris-HCl, pH 8.0, 50 mM KCl, 1 mM $MgCl_2$, 5 mM β-mercaptoethanol, 1 mM spermidine, 1 mM dGTP, 1 mM dTTP, 10 μM Cy5-dATP, 140 pM telomerase, and 100 nM primer concentration (unless otherwise mentioned). Significantly higher concentrations of Cy5-dATP were avoided to ensure unincorporated Cy5-dATP could be efficiently removed prior to single molecule measurements. Following incubation at 30 °C for 2.5 h, the reaction was stopped by adding 150 μL of TEN buffer (10 mM Tris-HCl, 10 mM EDTA, and 300 mM NaCl), and the mixture was extracted with equal volume of phenol/chloroform. The supernatant was applied to a G-25 spin column to remove excess nucleotides and dialyzed twice against 800 mL of autoclaved TEN buffers using MicroDispoDialyzer (MWCO 3.5 kDa, Spectrum Laboratories). Each experiment was performed in duplicate.

Direct Telomerase Activity Assay

Telomerase activity of immunopurified telomerase complex reconstituted in vitro in RRL was determined by a direct assay protocol modified from Chen et al.13 Briefly, telomerase was reconstituted using up to 200 μL of TNT-coupled RRL (Promega) according to the instructions of the manufacturer. The reconstituted active enzyme was affinity purified using a 40 μL suspension of anti-FLAG (M2 antibody) beads as described above. The telomerase elongation was performed in a total volume of 50 μL in 1 × telomerase reaction buffer (50 mM Tris-HCl, pH 8.0, 50 mM KCl, 1 mM $MgCl_2$, 5 mM β-mercaptoethanol, 1 mM spermidine) with 25.1 μCi of [α-^{32}P]-dGTP (3000 Ci/mmol), 20 μL of the telomerase/bead slurry, 1 μM of three-repeat primer $(TTAGGG)_3$, 0.5 mM dATP, 0.5 mM dTTP, 3 μM dGTP at 30 °C for 3 h. To the mixture, 50 μL of RNase stop solution (10 mM EDTA, 20 mM Tris-HCl, pH 8.0, 0.1 mg/mL RNase A (Roche), and 500 mM KCl) was added and kept at 37 °C for 15 min, and then 50 μL of Proteinase K solution (10 mM Tris-HCl, 0.5% w/v SDS, 0.3 mg/mL proteinase K (Roche)) was added for another 15 min. The mixture was then subject to phenol/chloroform extraction and ethanol precipitation overnight. After centrifuging, washing the resultant pellet with 70% ethanol followed by a second centrifugation, the pellet was dissolved in 20 μL of denaturing gelloading buffer (40% formamide, 10 mM Tris-HCl pH 8.0, 10 mM EDTA, 0.05% xylene cyanol), heated at 65 °C for 5 min, and then snap-cooled on ice. The entire sample was loaded onto a denaturing 10% polyacrylamide DNA sequencing gel (1 × TBE/8 M urea) and subjected to electrophoresis. The gel was dried and exposed for appropriate times. After scanning by PhosphorImaging (Molecular Dynamics), the densitometric analysis on each band was performed with the ImageQuant v.3.0 software. The resulting data for each band was normalized by dividing by the number of added repeats for that band to account for the differences in specific radioactivity for each telomeric extension product. The data were then fitted to the function $y = AX^{n-1}$, where A is the intensity of the first band, n is the number of added repeats for each band in the gel, and X is the mean processivity of the enzyme as defined in the data analysis section.

TCCD Apparatus

The apparatus for two-color single molecule fluorescence coincidence detection has been reported previously.18 Briefly, two overlapping laser beams (488 nm, Argon ion, model 35LAP321-230, Melles Griot, and 633 nm model 25LHP151 HeNe laser, Melles Griot) were directed through a dichroic mirror and oil immersion objective (Apochromat 60x, NA 1.40, Nikon). The beams were focused 5 μm into a 1 mL sample solution contained in a Lab-TeK chambered coverglass (Scientific Laboratory Suppliers Ltd., Surrey, UK). Fluorescence was collected by the same objective and imaged onto a 50 μm pinhole (Melles Griot) and sent to two avalanche photodiodes (APD) (SPCM AQ-161, EG&G, Canada).

Estimation of Telomerase Concentration by TCCD

Telomerase with Alexa-488-labeled hTR was purified using antibody immobilization and 3×FLAG elution as described above. The purified telomerase was subjected to single molecule measurement, and fluorescence bursts were collected and directly compared to that of a synthetic 100% Alexa-488 labeled 40-mer single-stranded DNA (ssDNA) at known concentration as a reference. The burst probability is proportional to the concentration of the molecule and its diffusion coefficient. Assuming that telomerase consists of two hTR and two hTERT, the calculated molecular weight is 554 kDa,22 while the 40-mer ssDNA has a molecular weight of 12 kDa. Since the diffusion coefficient is approximately inversely proportional to the cube root of the molecular weight, this gives a correction factor of 3.6, thus allowing the telomerase concentration to be estimated.

Detection of Telomerase Activity by TCCD

Following telomerase primer extension and purification as described above, the telomerase products were diluted to 50 pM of Alexa-488-labeled primer concentration in TEN buffer complemented with 0.01% Tween-20. The diluted sample was mixed and incubated at 20 °C for 10 min before measurements. For all the single molecule experiments, data were collected for 90 min at 20 °C with a 1 ms bin time on both MCS cards.

Data Analysis

Coincidence events, representing the number of product molecules, were selected by applying a threshold of 10 counts per ms for both channels. The total number of primer molecules was counted by applying the same threshold in the blue channel only. The distribution of product molecules was characterized by forming a histogram of the population density of the function Z on the coincidence data, where $Z = \ln(I_{red}/I_{blue})$. These histograms were then fitted by a sum of a series of Gaussian peaks, each peak corresponding to the population of DNA fragments with a particular extension number. Thus, the principal difference between these peaks is their position, which depends on the extension number. The distributions of fluorescence for each extension product both exceed a high threshold and are highly correlated. It was therefore found to be reasonable to estimate the mean position to be $\langle Z_n \rangle \approx 1n(n\langle I_{red}\rangle_f/\langle I_{blue}\rangle_f)$, where $\langle I \rangle_f$ is the brightness of the fluorophore specified and n is the extension number of the product, i.e., the number of telomeric repeats added. In addition there are two other differences between the peaks: their widths and their areas. The standard deviation of a peak corresponding to a product of extension number n is given by:

$$\sigma_n = \sqrt{\frac{K}{n\langle I_{red}\rangle_f} + \frac{K}{\langle I_{blue}\rangle_f}} \quad (1)$$

where it is assumed that the error in fluorophore emission is $\sqrt{K}$ times the shot-noise limit. The areas of the peaks are assumed to decrease in the geometric progression AX^{n-1}, where A is the area of the first peak, X is the mean processivity of the enzyme which is assumed to be the same for each repeat addition and $0 \leq X < 1$. This assumption is made to reduce the number of parameters in the fitting procedure. The number of independent parameters is further reduced by determining both the brightness of the fluorophores and the area of the first peak from the original coincidence data for a single extension product. For a given value of the variable X these parameters may be calculated by the following formulas:

$$A = E(1 - X) \quad (2)$$

where E is the total number of coincident events;

$$\langle I_{\text{blue}}\rangle_{\text{f}}=\langle I_{\text{blue}}\rangle_{\text{c}} \quad (3)$$

i.e. the brightness of the blue (reference) fluorophore is the same as the brightness of the blue channel, and

$$\langle I_{\text{red}}\rangle_{\text{f}}=\langle I_{\text{red}}\rangle_{\text{c}}\,(1-X) \quad (4)$$

where $\langle I_{\text{red}}\rangle_{\text{c}}$ is the brightness of the red channel.

Note that the brightness of the red channel will increase if a large fraction of extended products are formed which contain several fluorophores.

Equations 2 and 4 are derived from the series contractions

$$\sum_{1}^{N} AX^{n-1}=\frac{A}{1-X}=E \quad (5)$$

and

$$\langle I_{\text{red}}\rangle_{\text{c}}=\frac{1}{E}\sum_{1}^{N} n\langle I_{\text{red}}\rangle_{\text{f}}AX^{n-1}=\frac{A}{E}\frac{\langle I_{\text{red}}\rangle_{\text{f}}}{(1-X)^2} \quad (6)$$

In practice, K was estimated by fitting an initial set of data from a control sample with only one added repeat, where X could reasonably be assumed to be zero. The subsequent experimental histograms were fitted with K fixed to the value derived in this way $\left(\sqrt{K}=2.52\right)$. Thus, there was only one independent parameter, X. The reduced χ^2 values for fits obtained using this procedure were in the range 0.5-2.1.

For the model samples we found that the K values for the 1:1 and 2:1 samples were significantly different. This is possibly due to the two fluorophores being in different environments. For the mixture of the 1:1 and 2:1 DNA we obtained poor fits when we had the same fixed or variable value of K for both components, giving rise to a reduced population of 2:1 DNA. We therefore used the experimentally determined K values for the 1:1 and 2:1 sample to fit the logarithm of the ratio for the mixture. In this fitting the only variables were the relative populations of the two samples and the brightness of the red fluorophore. A detailed study on how the variation in the local environment of the fluorophore affects the K value will be the subject of future research.

The total product concentration C_{p} and product concentration of the ith peak $C_{\text{p}i}$ where i is the number of repeats added were calculated using the following equations:

$$C_{\text{p}}=4.0\cdot C_0\,(N_{\text{coin}}/N_{\text{blue}}) \quad (7)$$

$$C_{pi}=\frac{C_{\text{p}}\cdot X^{i-1}}{1-X} \quad (8)$$

where N_{coin} and N_{blue} represents the number of coincidence events and blue fluorescent bursts, C_0 is the initial primer concentration, 4.0 is the experimentally determined correction factor for the coincidence detection efficiency for our setup, determined using the Cy5-Alexa-488 dsDNA sample as control.

Results

Experimental Design to Measure Telomerase Activity

The concept (Figure 2) relies on the use of a three-repeat primer substrate $(TTAGGG)_3$, pre-labeled with a reference fluorophore (Alexa-488). Primer elongation was initiated with the addition of dTTP, dGTP, and Cy5-dATP, such that telomerase incorporated one Cy5-dATP per telomeric repeat. The telomeric DNA extension products were purified and then subjected to single molecule measurements at 50 pM total DNA concentration. Two different laser beams were focused into the probe volume to independently excite the two fluorophores. The excitation powers were adjusted so that the mean intensities of red and blue fluorescence for single fluorophores were approximately equal. The DNA products containing both fluorophores diffused through the probe volume and generated fluorescence bursts simultaneously in both channels, giving rise to coincidence events. However, unextended primers only gave rise to fluorescent bursts in the blue channel (Alexa-488). By directly counting the number of coincident events and independently measuring the coincidence detection efficiency, one can directly determine the number of extended products formed. By determining the ratio of the intensity of the Alexa-488 fluorophore to that of the Cy5 and analyzing the resulting distribution it is possible to determine the relative populations of the different extended products, and hence the concentration of individual products and thus the processivity of the enzyme.

Estimation of Telomerase Concentration

Telomerase was reconstituted in the presence of 3×FLAG-tagged hTERT and Alexa-488-labeled hTR. The tag affinity-purified telomerase was subjected to single molecule measurement. Direct comparison of the fluorescence burst count rate with that of a synthetic 100% Alexa-488 labeled 40-mer DNA, of known concentration, allowed for the concentration of Alexa-488-labeled telomerase complex to be estimated as 7 ± 1 nM.

Fitting of Logarithmic Ratio Histograms Using Gaussian Distributions

In these experiments the two types of fluorophores on the extended products were excited independently, and the fluorescence from each was detected on separate avalanche photodiodes. Coincident bursts were selected by determining times when both channels exceeded a background threshold, and the ratios of these counts were then calculated. After taking the logarithms of these ratios the resulting numbers were used to form a histogram with constant bin widths. These histograms were then fitted using Gaussian distributions. If we were to retransform the data to form the probability density of the straight ratio, I_{red}/I_{blue}, then these distributions would be transformed into log-normal functions. Log-normal functions are widely used where two effects combine in a multiplicative rather than additive fashion23 (see Supporting Information for justification). However, it is more convenient to deal with constant bin widths and Gaussian distributions and fit the histogram of logarithmic ratios. To validate this approach to fitting the data, we first made two model dsDNA samples; one sample had a single Rhodamine Green and Alexa-647 fluorophore (1:1 labeled dsDNA), and the second had one Rhodamine Green and two Alexa-647 fluorophores (2:1 labeled dsDNA). The laser powers were adjusted so that the fluorescence intensity from a single Rhodamine Green and Alexa-647 fluorophore were approximately equal. Figure 3A shows the experimental ratio histogram for the 1:1 labeled dsDNA. These data are clearly asymmetric and hence will be poorly fitted by a Gaussian. Figure 3B shows the fit of the logarithm of the ratio for the same control sample. This is well fitted by a normal distribution centered close to zero. Figure 3C shows the fit of the logarithm of the ratio for the model 2:1 labeled sample. This is again well fitted by a Gaussian distribution but is now centered close to 0.7 (i.e., [ln 2]), as expected. We then examined a model mixture of equimolar 1:1 and 2:1 labeled dsDNA (Figure 3D). The distribution of the logarithm of the

ratio for this mixture is well fitted by the sum of the distributions of logarithms of the ratios obtained from the 1:1 and 2:1 labeled samples, as expected, with 48% ± 7% 1:1 sample and 52% ± 7% 2:1 sample. We also used our analysis method to fit the distribution of the logarithm of the ratio measured for the mixture, assuming the fluorescence from the Alexa-647 in the 2:1 sample is twice that of the 1:1 sample, and hence determined the relative populations of the individual 1:1 and 2:1 labeled components (see Experimental Section for details). We recovered populations of 49% ± 8% and 51% ± 8%, respectively, in excellent agreement. This shows that the logarithmic ratio histogram can be fitted to recover accurate populations of components each with different ratios of fluorophores.

Determination of Relative Product Populations and Mean Processivity for Wild-Type Telomerase and Mutant

To determine the relative populations of the extended products of the telomerase reaction, the logarithmic ratio histogram was fitted with a series of Gaussian distributions. We have assumed that the nth repeat is n times brighter than a single repeat, and a control sample, with only one repeat added, was employed to determine the value of the parameter K from the width of the peak (Figure 4A) (K defines the intensity fluctuation of a single fluorophore in the extended product and hence determines the peak width). We assumed that the intensity fluctuations of each fluorophore are independent, so the width of the nth peak, in a logarithmic ratio plot, is a function of both n and K (see Experimental Section for details). Given that each incorporated fluorophore is expected to be in the same local environment, we assumed K is the same for each repeat. Using the predetermined value of K from the reference sample means that the fitting of the logarithm of the ratio for extension products has only one adjustable parameter, which is the mean processivity, X.

Figure 4C shows a representative histogram for the analysis of extension products of wild-type telomerase. Each population (n = 1, n = 2, n = 3, etc.) represents extension products with n added repeats as shown in the bar chart in Figure 4D. Experiments were performed over a range of telomerase concentrations from 50 pM to 1.4 nM, and no concentration dependence of the processivity was found. The average processivity value, over this concentration range, was 0.32 ± 0.04 for the wild-type enzyme. We performed the same analysis on a telomerase mutant enzyme (described in detail later) at 140 pM concentration, as shown in Figure 4B, which gave a smaller number of coincident events and did not yield significant populations of extension products. Fitting of the histogram gave a processivity value of $X = 0.04 \pm 0.04$

Validation of Method

To address the assumptions made in our analysis of the single molecule telomerase data, we independently analyzed wild-type human telomerase activity using a direct radioactivity assay.12-14 Here we expressed and purified sufficient wild-type enzyme, then carried out extension in the presence of [α-^{32}P]dGTP, and separated the extension products by gel electrophoresis. Figure 5A shows a typical profile of extension products visualized on a phosphorimager, and the resulting data was fit to $y = AX^{n-1}$, where A is the intensity of the first band, n is the number of repeats added for a given band in the gel, and X is the mean processivity of the enzyme as defined in the data analysis section. A representative fit is shown in Figure 5B. Analysis of three independent measurements gave a mean processivity of 0.37 ± 0.05, which is in good agreement with the value of 0.32 ± 0.04 derived from the single molecule telomerase assay. This supports that the single molecule method and data analysis faithfully report on the activity profile of telomerase.

Detection and Quantitation of Telomerase Catalytic Activity by TCCD

The results of the experiments on wild-type telomerase are shown in Figure 6. There was a linear relationship between telomerase concentration and either the total concentration of product molecules or the total concentration of repeats added, up to 140 pM, but the correlation started to flatten beyond 140 pM (the total concentration of repeats was calculated from the concentration of products and the processivity at each telomerase concentration).

At 140 pM telomerase and 100 nM initial substrate the total product concentration was 12.8 ± 1.0 nM after 150 min. If one assumes all telomerase enzyme complexes are fully active and saturated by substrate molecules (DNA primer and dNTPs), each telomerase molecule must be turning over at least 90 substrate molecules in 150 min, suggesting a lower limit for the enzyme turnover rate of 0.60 substrates min^{-1}. Processive telomerase can add multiple DNA repeats to each substrate prior to dissociation (i.e., turnover). The total concentration of repeats added by 140 pM of telomerase in 150 min was 22 ± 3 nM, suggesting a lower limit for the enzymatic repeat addition of 1.0 repeats min^{-1} under these conditions. The rate of nucleotide polymerization under these specific conditions was calculated to be 6.0 nucleotides min^{-1} on average.

Case Study of a Telomerase Template Mutant

To further demonstrate the utility of the single molecule approach for profiling telomerase activity, we examined a mutant with altered activity. The template domain of hTR comprises 11 residues (3′-CAAUCCCAAUC-5′), which may be functionally divided into two distinct regions known as the alignment and elongation domains.13,20,24 The alignment domain has been postulated to function to reposition the primer substrate by DNA-RNA base pairing during processive synthesis (Figure 1). Previously we have suggested that substitution, or deletion, of one or two nucleotides from the 3′-end of the alignment domain of hTR causes a slight reduction in telomerase activity with negligible change in processivity of telomerase. 20 As part of the same study, deletion or substitution of three or more residues from the 3′-end of the alignment domain resulted in total loss of telomerase activity as judged by the PCR-based TRAP assay.20 However, we were not able to rule out the possibility of nonprocessive catalytic activity, leading to short extension products undetectable by TRAP. Here we have reevaluated one of the key, apparently inactive, mutants using the single molecule approach. Specifically, the Sub3 mutant (^{56}CAA^{54} substituted by GTT) was chosen for this study. Figure 4B shows the data for the mutant telomerase, and quantitative analysis showed that the total product concentration was 4.5 ± 0.5 nM and the total concentration of repeats added was 4.8 ± 0.7 nM. Thus, the total product and repeat concentrations have been reduced to 35% and 22%, respectively, relative to wild-type telomerase. Importantly, the TCCD method found the mutant telomerase to be nonprocessive (processivity value 0.04 ± 0.04).

Discussion

Measurements on Wild-type Human Telomerase

We have used TCCD to detect extended products of telomerase in the presence of an excess of unextended products, where the fraction of primers extended was typically only 4%. We have extended TCCD to analyze the logarithmic ratio histograms of molecules with multiple numbers of just one of the two fluorophores. Model samples confirmed that relative populations could be determined by fitting using Gaussian distributions. This method has then been used to measure the turnover and processivity of reconstituted recombinant human telomerase. The enzyme was found to be processive, as anticipated based on TRAP assay25,26 and direct primer extension assay.11,13 We considered the possibility of self-

quenching between multiple incorporated Cy5 dyes, which would lead to a substantial reduction in the apparent processivity measured by TCCD. To address this we carried out an independent measurement of telomerase processivity using the direct radioactivity assay. The processivity values obtained by both methods are in excellent agreement, suggesting that there is no significant self-quenching in this method. Furthermore, this agreement also supports the assumption that similar K values for the different telomerase extension products is valid. The dependence of catalytic activity with telomerase concentration is linear up to 140 pM, but flattens above 140 pM (Figure 6 A and B). This may reflect reduced activity caused by a higher aggregation state of telomerase at higher concentration. The assay is sufficiently sensitive to detect 50 attomoles of product molecules extended by 105 molecules of telomerase, which is comparable with other PCR-independent methods.[15,27-29]

By directly counting the number of telomerase enzyme complexes we have determined the turnover number per molecule of telomerase as 0.60 substrate min^{-1} and the average nucleotide incorporation rate as 6.0 nucleotides min^{-1}. These must be regarded as a lower limit since (a) we cannot rule out the possibility that less than 100% of the telomerase molecules are catalytic active, and (b) the method involves incorporation of a nonnatural nucleotide. The estimated nucleotide incorporation rate (6.0 nucleotides min^{-1}) is comparable to that of other DNA polymerases such as Klenow polymerase (3.6 nucleotides/min^{-1}),[30] HIV-1 reverse transcriptase (6 nucleotides/min^{-1}), and T7 polymerase (7.2 nucleotides/min^{-1}),[31] under single nucleotide incorporation and steady-state conditions, where DNA dissociation is rate limiting.

Characterization of a Telomerase Template Mutant

In our previous studies we systematically deleted or substituted nucleotides within the alignment domain of hTR to determine their specific role in telomerase catalysis.[20] The original data, obtained using the PCR-based TRAP method, suggested that the apparent minimal length requirement of the alignment domain is 3 nucleotides, with the caveat that catalytic activity resulting from a mutant with low processivity (i.e. less than 3 repeats) would be undetectable. Using TCCD, we have specifically reinvestigated the case of the Sub3 telomerase mutant (^{56}CAA^{54} in the alignment domain substituted by GTT). Our new data demonstrated that the Sub3 mutant was in fact catalytically active but has no measurable repeat addition processivity, in contrast with mutants having only a single (Sub1) or double (Sub2) mutation, and also wild-type enzyme which retain their processive mechanisms.[20] The repeat addition processivity of telomerase involves both a transient dissociation and re-alignment of telomeric DNA (Figure 1).[6] The observation of an active but nonprocessive mutant (Sub3) results from a decrease in the k_{trans}/k_{off} ratio (Figure 1). That the two nucleotides, ^{52}C^{53}U at the 3′-end of the template are sufficient for catalytic activity is consistent with the observation that eight nucleotides in the template region are absolutely conserved among all known vertebrate telomerase RNA.[24] This new result has prompted a comprehensive study on the alignment domain of human telomerase using TCCD that will be the subject of a separate paper in due course.

Conclusion

By extending TCCD to deal with a mixture of extension products with multiple fluorophores, we have opened up an important and nonclassical enzyme system for detailed quantitative studies. In addition to the advantages of high sensitivity and the avoidance of radioactivity, the mechanism of human telomerase is able to be profiled in ways that have proved difficult using classical methods. This study shows the power of adapting single molecule methods for the study of biomolecular systems, and will be employed going forward to provide further fundamental insights into the mechanism of telomerase and of

telomerase inhibitors. This new method of analysis can also be used more generally to study the stoichiometry of complexes or oligomers of other fluorophore-labeled biomolecules, in the presence of an excess of unassociated biomolecules without any separation, which will enable new biomolecular questions to be addressed in the future.

Acknowledgments

We thank the BBSRC for funding. We also thank Dr. Gerald Gavory for stimulating discussions and Dr. James Redman and Dr. Angel Orte for proofing the manuscript.

References

(1). Kim NW, Piatyszek MA, Prowse KR, Harley CB, West MD, Ho PL, Coviello GM, Wright WE, Weinrich SL, Shay JW. Science. 1994; 266:2011–2015. [PubMed: 7605428]

(2). Collins K, Mitchell JR. Oncogene. 2002; 21:564–579. [PubMed: 11850781]

(3). Vulliamy T, Marrone A, Goldman F, Dearlove A, Bessler M, Mason PJ, Dokal I. Nature. 2001; 413:432–435. [PubMed: 11574891]

(4). Wong JM, Collins K. Lancet. 2003; 362:983–988. [PubMed: 14511933]

(5). Chen JL, Greider CW. Trends. Biochem. Sci. 2004; 29:183–192. [PubMed: 15082312]

(6). Kelleher C, Teixeira MT, Forstemann K, Lingner J. Trends. Biochem. Sci. 2002; 27:572–579. [PubMed: 12417133]

(7). Lue NF. Bioessays. 2004; 26:955–962. [PubMed: 15351966]

(8). Kim NW, Wu F. Nucleic Acids Res. 1997; 25:2595–2597. [PubMed: 9185569]

(9). Krupp G, Kuhne K, Tamm S, Klapper W, Heidorn K, Rott A, Parwaresch R. Nucleic Acids Res. 1997; 25:919–921. [PubMed: 9016650]

(10). Wu YY, Hruszkewycz AM, Delgado RM, Yang A, Vortmeyer AO, Moon YW, Weil RJ, Zhuang Z, Remaley AT. Clin. Chim. Acta. 2000; 293:199–212. [PubMed: 10699434]

(11). Huard S, Moriarty TJ, Autexier C. Nucleic Acids Res. 2003; 31:4059–4070. [PubMed: 12853623]

(12). Morin GB. Cell. 1989; 59:521–529. [PubMed: 2805070]

(13). Chen JL, Greider CW. EMBO. J. 2003; 22:304–314. [PubMed: 12514136]

(14). Patolsky F, Gill R, Weizmann Y, Mokari T, Banin U, Willner I. J. Am. Chem. Soc. 2003; 125:13918–13919. [PubMed: 14611202]

(15). Maesawa C, Inaba T, Sato H, Iijima S, Ishida K, Terashima M, Sato R, Suzuki M, Yashima A, Ogasawara S, Oikawa H, Sato N, Saito K, Masuda T. Nucleic Acids Res. 2003; 31:E4–4. [PubMed: 12527793]

(16). Weizmann Y, Patolsky F, Lioubashevski O, Willner I. J. Am. Chem. Soc. 2004; 126:1073–1080. [PubMed: 14746475]

(17). Weiss S. Science. 1999; 283:1676–1683. [PubMed: 10073925]

(18). Li HT, Ying LM, Green JJ, Balasubramanian S, Klenerman D. Anal. Chem. 2003; 75:1664–1670. [PubMed: 12705600]

(19). Dahan M, Deniz AA, Ha TJ, Chemla DS, Schultz PG, Weiss S. Chem. Phys. 1999; 247:85–106.

(20). Gavory G, Farrow M, Balasubramanian S. Nucleic Acids Res. 2002; 30:4470–4480. [PubMed: 12384594]

(21). Ren XJ, Gavory G, Li HT, Ying LM, Klenerman D, Balasubramanian S. Nucleic Acids Res. 2003; 31:6509–6515. [PubMed: 14602909]

(22). Wenz C, Enenkel B, Amacker M, Kelleher C, Damm K, Lingner J. EMBO J. 2001; 20:3526–3534. [PubMed: 11432839]

(23). Limpert E, Stahel W, Abbt M. Bioscience. 2001; 51:341–352.

(24). Chen JL, Blasco MA, Greider CW. Cell. 2000; 100:503–514. [PubMed: 10721988]

(25). Weinrich SL, et al. Nat. Genet. 1997; 17:498–502. [PubMed: 9398860]

(26). Beattie TL, Zhou W, Robinson MO, Harrington L. Curr. Biol. 1998; 8:177–180. [PubMed: 9443919]

(27). Grimm J, Perez JM, Josephson L, Weissleder R. Cancer Res. 2004; 64:639–643. [PubMed: 14744779]

(28). Lackey DB. Anal. Biochem. 1998; 263:57–61. [PubMed: 9750143]

(29). Xu SQ, He M, Yu HP, Wang XY, Tan XL, Lu B, Sun X, Zhou YK, Yao QF, Xu YJ, Zhang ZR. Clin. Chem. 2002; 48:1016–1020. [PubMed: 12089169]

(30). Kuchta RD, Mizrahi V, Benkovic PA, Johnson KA, Benkovic SJ. Biochemistry. 1987; 26:8410–8417. [PubMed: 3327522]

(31). Furge LL, Guengerich FP. Biochemistry. 1997; 36:6475–6487. [PubMed: 9174365]

Europe PMC Funders Author Manuscripts

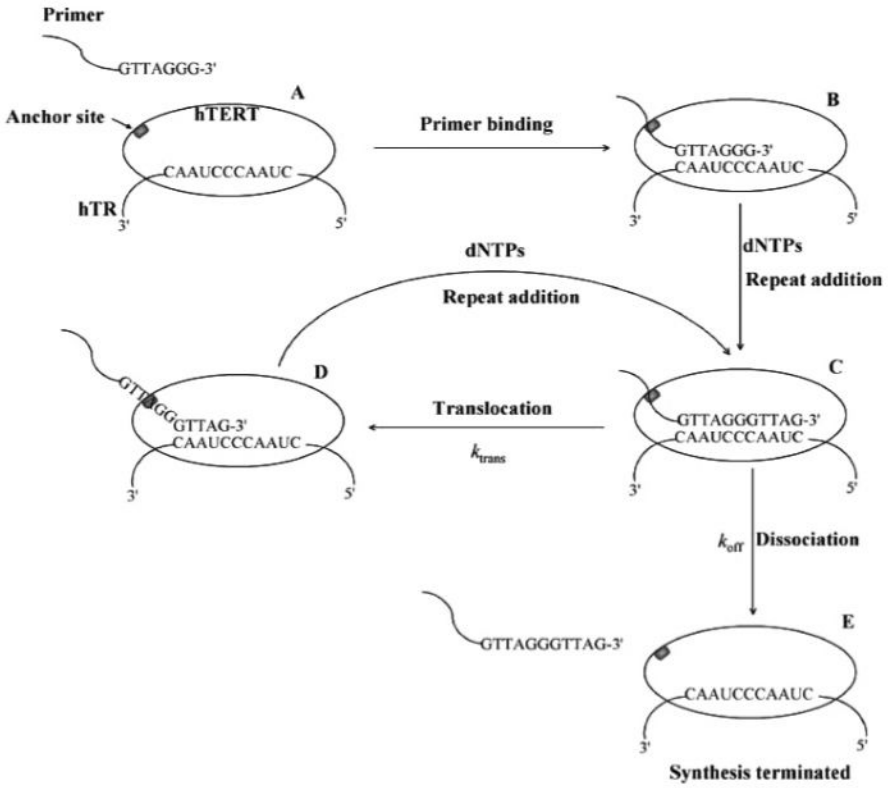

Figure 1.

Proposed molecular mechanism of human telomerase-catalyzed synthesis of telomere DNA. (A) Telomerase catalytic protein (hTERT) is shown with the template sequence spanning nucleotides +46 to +56 of the RNA subunit (hTR) and the anchor site of the hTERT subunit. The DNA primer is shown with 3′-end sequence 5′-GTTAGGG-3′. (B) DNA primer binds to telomerase by base pairing with the template region of telomerase RNA, plus additional interactions between primer and the hTERT anchor site. (C) Telomerase extends the telomeric primer by the addition of complementary dNTPs. (D) Following translocation, the DNA primer is in position for further rounds of extension. (E) The extended DNA primer dissociates from its active site.

Europe PMC Funders Author Manuscripts

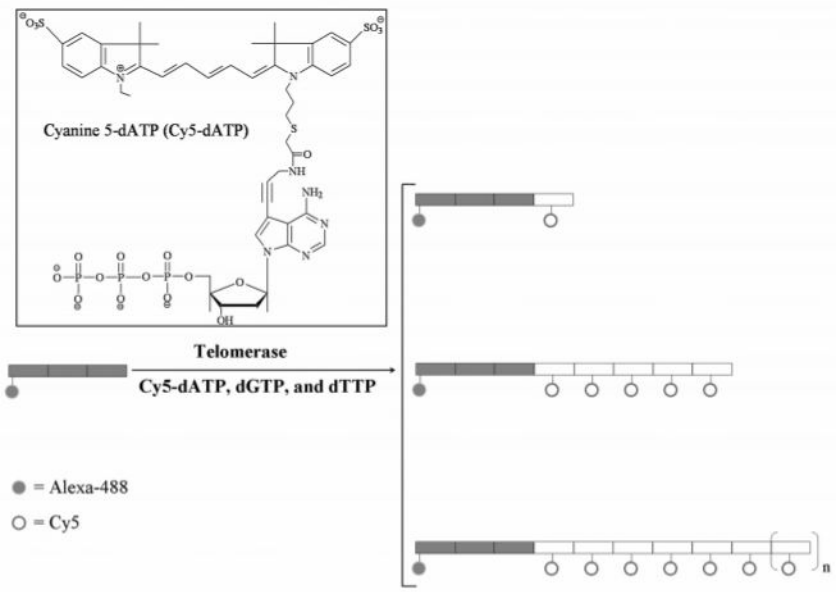

Figure 2.

Three-repeat DNA primer, pre-labeled with Alexa-488, is extended by telomerase in the presence of Cy5-dATP, dGTP, and dTTP. During primer elongation, telomerase incorporates only *one* Cy5-dATP per telomeric repeat (TTAGGG) synthesized. (Inset) Structure of Cy5-dATP.

Europe PMC Funders Author Manuscripts

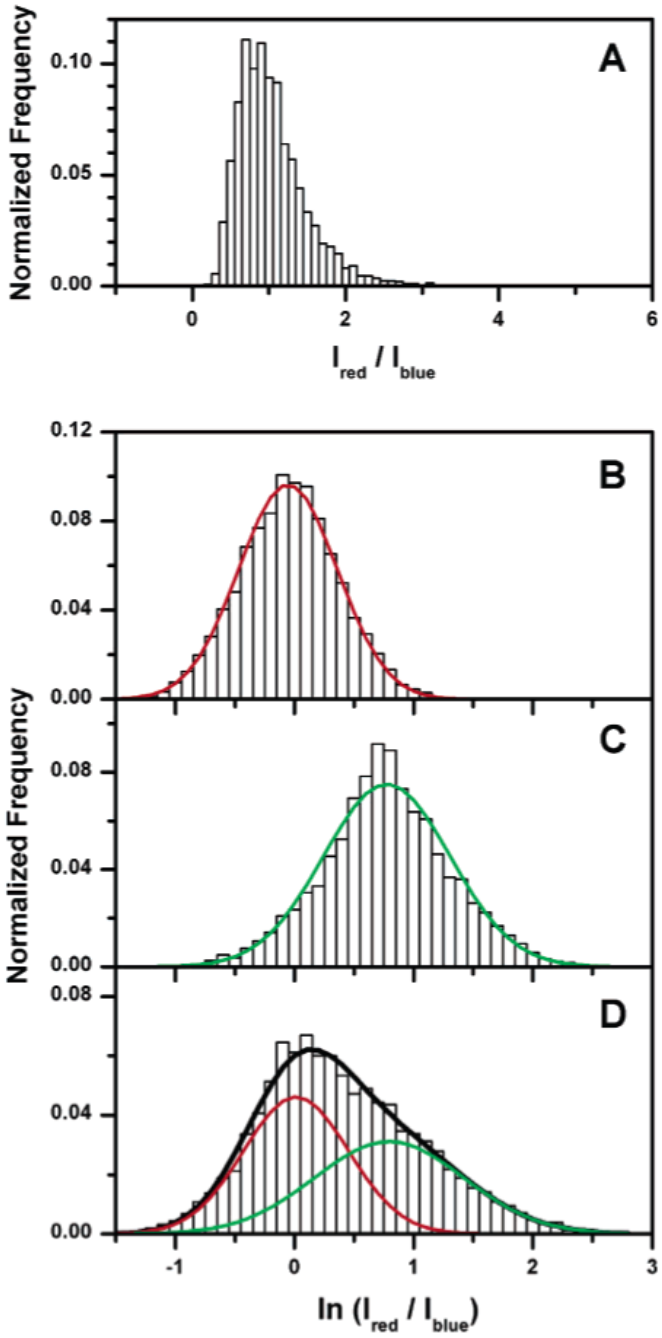

Figure 3.

Fitting of histograms for dsDNA model samples labeled in 1:1 and 2:1 stoichiometries with Rhodamine green and Alexa-647. (A) Histogram of ratios for the 1:1 dsDNA model sample is asymmetric and does not fit to a single Gaussian distribution. (B) Histogram of the logarithms of ratios for the same 1:1 dsDNA model sample data (11429 coincident events) is well fitted by a single Gaussian distribution (red line) with one fitted parameter: $\sqrt{K}=1.52$. The experimentally derived fluorophore brightnesses were 27.8 counts ms^{-1} and 26.3 counts ms^{-1} for Rhodamine green and Alexa-647, respectively. (C) Histogram of logarithms of ratios for the 2:1 dsDNA model sample data (10746 coincident events) is well fitted by a

single Gaussian distribution (green line) with one fitted parameter: $\sqrt{K}$=2.16. The experimentally derived fluorophore brightnesses were 24.3 counts ms^{-1} and 26.3 counts ms^{-1} for Rhodamine green and Alexa-647, respectively. (D) Distribution over 12158 coincident events observed for an equimolar mixture of the 1:1 and 2:1 dsDNA samples and the fitted distribution using two Gaussians. The black, red, and green lines are the fitted distributions for the mixture, 1:1 component and 2:1 component, respectively. The two fitted parameters were the brightness of the Alexa-647 fluorophore (23.5 counts ms^{-1}) and the relative population of monomer (49% ± 8%) to dimer (51% ± 8%). The experimentally derived brightness of the Rhodamine green fluorophore was 23.3 counts ms^{-1}, and $\sqrt{K}$ was fixed at 1.52 and 2.16 for the monomer and the dimer distributions, respectively.

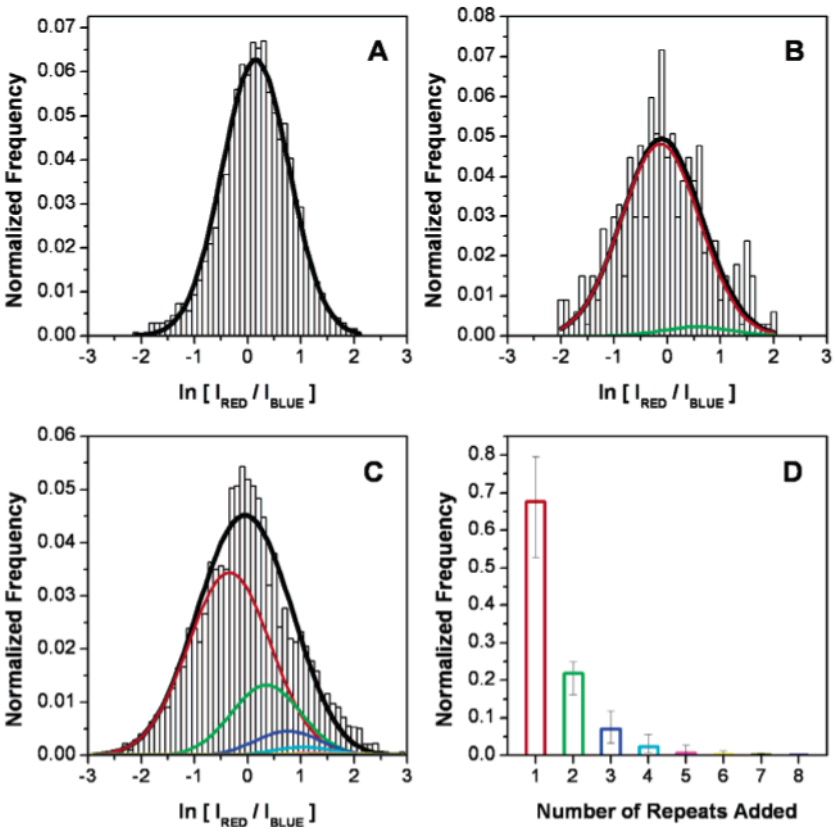

Figure 4.

Fitting of histograms of dual fluorophore-labeled extension products. Underlying populations (B and C) for different number of repeats added (D) are indicated by colored lines with the black line representing the overall distribution. (A) Cy5-Alexa-488 single-repeat extension product. The distribution over 2991 coincident events is fitted by a single parameter, $\sqrt{K}$=2.52 (the fluorophore brightnesses were 29.7 counts ms^{-1} and 34.6 counts ms^{-1} for Alexa-488 and Cy5, respectively). (B) Extended products from 140 pM mutant telomerase enzyme. The distribution over 333 coincident events is fitted by the processivity parameter at X = 0.04 ± 0.04 (the fluorophore brightnesses were 25.3 counts ms^{-1} and 22.1 counts ms^{-1} for Alexa-488 and Cy5, respectively, and $\sqrt{K}$ was fixed at 2.52 from the initial single extension product data). (C) Extension products with 700 pM wild-type telomerase. The distribution over 4718 coincident events is fitted by a single variable parameter, the processivity, X = 0.32 ± 0.13 (the fluorophore brightnesses were 25.7 counts ms^{-1} and 18.3 counts ms^{-1} for Alexa-488 and Cy5, respectively, and $\sqrt{K}$ was fixed at 2.52 from the initial single extension product data). The histogram is shifted on the horizontal axis since the laser powers used in this experiment resulted in unequal individual fluorophore brightness. The reduced χ^2 value for this fit is 2.12. (D) Bar chart showing extension product populations obtained from (C).

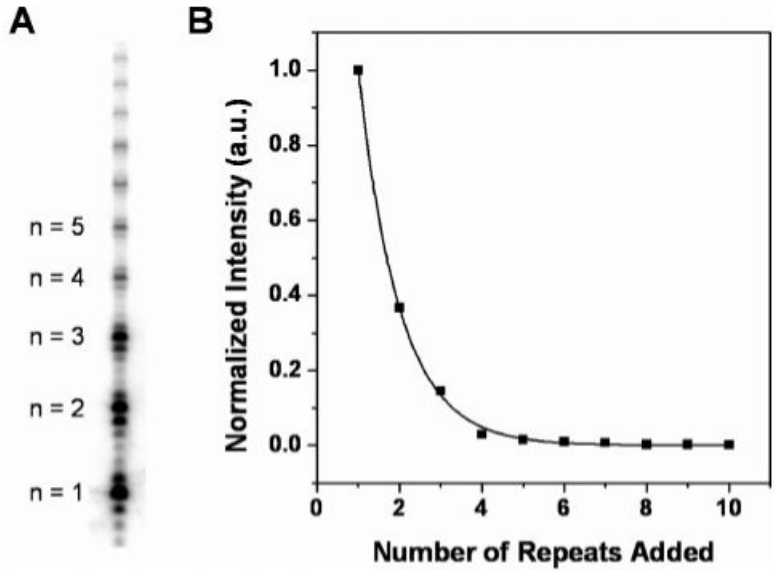

Figure 5.

Analysis of wild-type telomerase processivity by a direct radioactivity based assay. (A) Gel showing bands representing the extension products of the telomerase reaction. (B) Result of fitting the gel data based on the function $y = AX^{n-1}$, where A is the intensity of the first band, n is the number of repeats added for a given band in the gel, and X is the mean processivity of the enzyme as defined in the data analysis section. Intensities from each band in (A) were divided by the number of repeats in the extended products to normalize for the number of equivalents of radioactivity incorporated. The mean processivity derived from the fit is 0.37 ± 0.01.

Europe PMC Funders Author Manuscripts

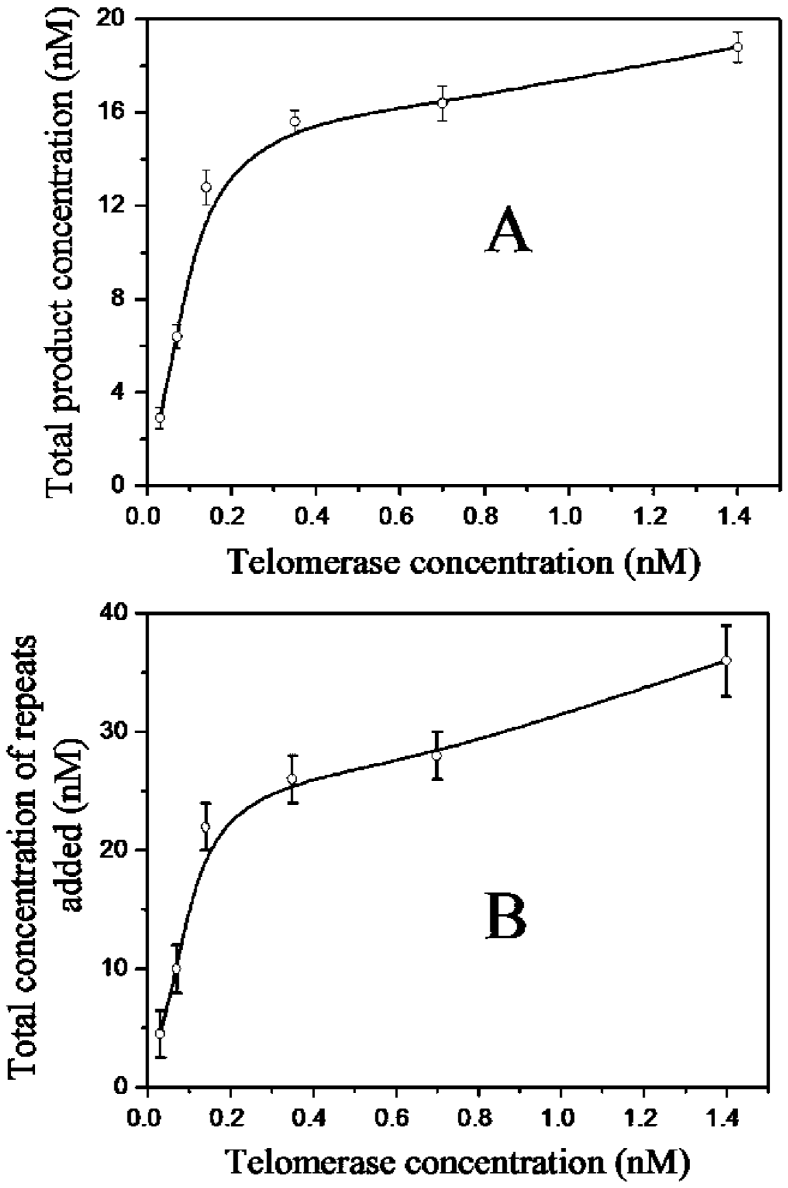

Figure 6.
Effect of wild-type telomerase concentration on: (A) the total product concentration, (B) total concentration of repeats added.